Int. J. Heat Mass Transfer. Vol. 25, No. 6, 823–834, 1982
Printed in Great Britain

0017-9310/82/060823-12 $03.00/0
Pergamon Press Ltd.

THE USE OF HEAT TRANSFER PRINCIPLES IN DESIGNING OPTIMAL DIATHERMY AND CANCER TREATMENT MODALITIES

ASHLEY F. EMERY and K. MICHAEL SEKINS
Department of Mechanical Engineering, University of Washington, Seattle, WA 98195, U.S.A.

(*Received* 16 *December* 1981)

Abstract—An experimental and numerical study of the thermal response of the human thigh exposed to diathermy treatments is described. By properly varying the simulation parameters and the temperature–blood flow model it is possible to obtain good agreement between the predicted and measured temperatures and blood flow rates. The simulation technique can then be used to predict the response of living tissue to a variety of treatment protocols. An example is given of the application of the method for the definition of the correct diathermy dose for tumor treatment.

NOMENCLATURE

BFR,	blood flow rate (abbreviation);
c,	specific heat capacity;
EM,	electromagnetic wave;
f,	mass specific blood flow rate;
h,	surface heat transfer coefficient;
M,	basal metabolic heat generation rate;
MBF,	muscle blood flow (abbreviation);
q''',	volumetric heat generation rate;
RBF,	resting (basal) blood flow rate abbreviation);
SAR,	specific energy absorption rate (abbreviation);
t,	time;
T,	temperature;
ρ,	density.

Subscripts

a,	arterial;
b,	blood;
d,	diathermy;
f,	fat;
s,	skin surface.

INTRODUCTION

ONE OF the effective treatment modalities of physical medicine is the use of diathermy heating to increase local tissue temperature. The primary rationale for the therapeutic heating is the inducement of blood flow changes which are expected to occur with an increase of local tissue temperature. Figure 1 illustrates a typical transient tissue temperature profile. Shortly after the temperature has reached a value in the neighborhood of 42°C, called the critical temperature, a rapid reduction to an equilibrium value is found [1]. This reduction is due to a substantial increase in the local blood perfusion rate. The therapeutic mechanism of the increased blood flow is thought to be associated with the increased supply of nurturing substances (e.g. oxygen, leukocytes, nutrients etc.) to the damaged tissue as well as the removal of toxic waste and cellular debris. In addition to perfusion changes, concomitant therapeutic effects produced by the direct action of temperature upon cellular and reflex functions are also expected.

The site of the pathology often requires that localized, deep volumetric heating methods be used, techniques collectively known as diathermy and effected by the deposition of microwave, shortwave or ultrasonic energy in the tissue. These techniques are often employed for such diverse conditions as: (1) relief of muscle, back, spine and joint pain; (2) reduction of muscle contraction; (3) increase of tissue extensibility to restore motion; (4) mitigation of arterial vascular insufficiency.

In addition, diathermy is being used in the treatment of cancer by: (1) direct thermal destruction of thermosensitive tumors; (2) augmentation of anti-cancer drugs by preferential heating of the malignant tissue [2, 3].

The dependence of the blood flow upon the tissue temperature is the basis of diathermy therapy, but one of the primary reasons that it is difficult to control and evaluate. The range between therapeutic and toxic temperatures is narrow [4] and the effectiveness of the

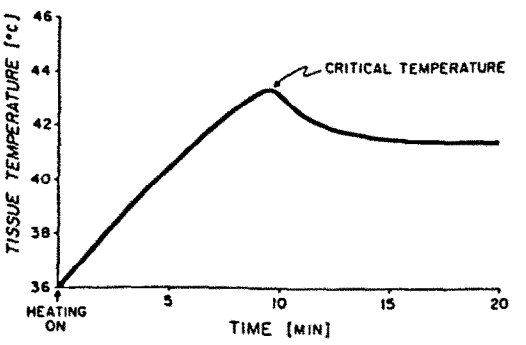

FIG. 1. The transient critical temperature behavior observed in diathermically heated tissues.

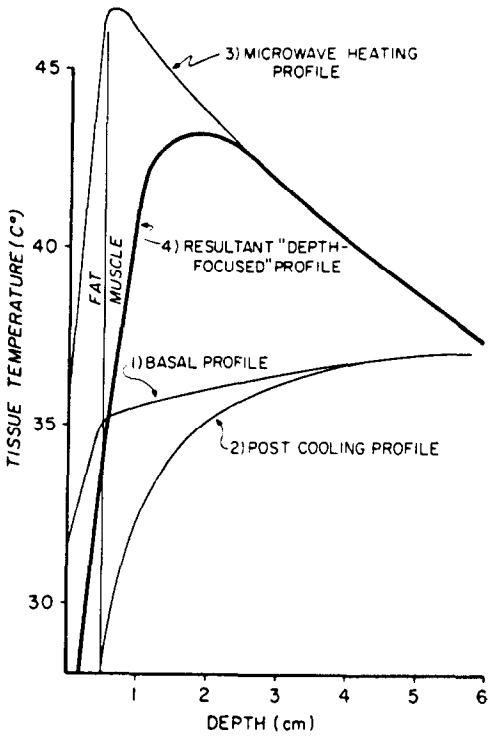

FIG. 2. Schematic of the temperature curves associated with the diathermy regime employing microwave heating and simultaneous surface cooling.

method often requires that the elevated temperature region be small. The thermoregulatory mechanisms which control blood flow, while extensively studied, are insufficiently understood to provide accurate predictions of local blood flow. Unfortunately, the convective heat transfer between the tissue and the blood dominates the body's thermal state and uncertainty about the rate of blood flow and the arterial heat transfer coefficient confuses the prediction of diathermy effects. Furthermore, the most complete studies are concerned with either whole body cardiac output or with local skin perfusion rates, not local deep tissue or muscle blood flow characteristics.

It has been demonstrated that heating of the superficial tissue produces only mild physiological reactions and few therapeutic effects [5]. For therapeutic potency, the diathermy treatment should apply heat preferentially to deeper tissues. This can be done by focusing the electromagnetic or acoustic waves or by cooling the skin surface. This surface cooling depresses the superficial temperatures, prevents the high temperatures which would otherwise occur at the muscle-fat interface and effectively shifts the heating to the deeper tissues. Figure 2 illustrates this effect [6]. Because of the different electrical properties of the fat and the muscle, the microwave deposition is a maximum at the fat-muscle interface [7]. When combined with the relatively high basal temperature at this point, the result may be a biologically damaging temperature level when the deposition rate is sufficient to produce therapeutic temperatures in the interior (e.g. 3-5 cm). By pre-cooling the surface, the pre-treatment temperature is reduced (curve 2) and the resulting temperature profile (curve 4) is acceptable and has a maximum shifted towards the deeper tissues.

Because of the interdependence of the temperature and the blood flow-itself a poorly defined physiological phenomenon — and the dependence of the temperature upon the energy deposition pattern, both the temperature-perfusion relationship and the energy deposition must be determined with reasonable accuracy. If this can be done, and if numerical techniques can predict the temperatures and blood flow, then it may be possible to analytically estimate the treatment protocol necessary for different injuries or tumors.

This paper is a description of an experimental and numerical study of the use of a 915 MHz direct contact diathermy applicator (Fig. 3) to produce elevated temperatures in the deeper muscle layers of the thigh [8]. The following sections discuss: the basic thermal characteristics of muscle tissue; the measurement of and modelling of the blood flow-temperature relationship; the measurement of transient temperature histories of a muscle treated by diathermy; and the numerical estimation of the temperature and comparison with the measured values. It is shown that numerical methods can be used to develop temperature blood flow models and to predict the effects of specified treatment protocols. It is also shown how this simulation may be used to design methods to treat tumors.

Before describing the results of the simulation, it is worthwhile to comment on the basic features of the thermal model. The analysis is made by using a standard finite element thermal analyzer with a source term at each node to represent the metabolic heat generation and the energy supplied by the arterial blood flow. The metabolic generation is varied with tissue temperature according to van't Hoff's law [9], which for biological tissue is often approximated by

$$\dot{M} = \dot{M}_0(1.1)^{\Delta T}. \tag{1}$$

The energy convected by the arterial blood is expressed as [10]

$$f\rho_b c_b(T_{in} - T_{exit}) \tag{2}$$

where f is the blood flow rate, T_{in} is the entering blood temperature, and T_{exit} is the venous return temperature. Because the heat exchange takes place in the smallest blood vessels, the capillaries, arterioles and venules, the heat exchanger effectiveness is essentially unity and the blood exits at the local tissue temperature [11] if the tissue volume is sufficiently large, usually taken to be greater than 0.1 mm^3 [12]. The entering blood temperature is usually lower than the body core temperature because of heat exchange while the blood is passing through the arterial tree, especially the intermediate portion [11]. As a result, it is usually assigned a value in the neighborhood of 36.25-36.5 C, as compared with the body core temperature of 37.6 C [13].

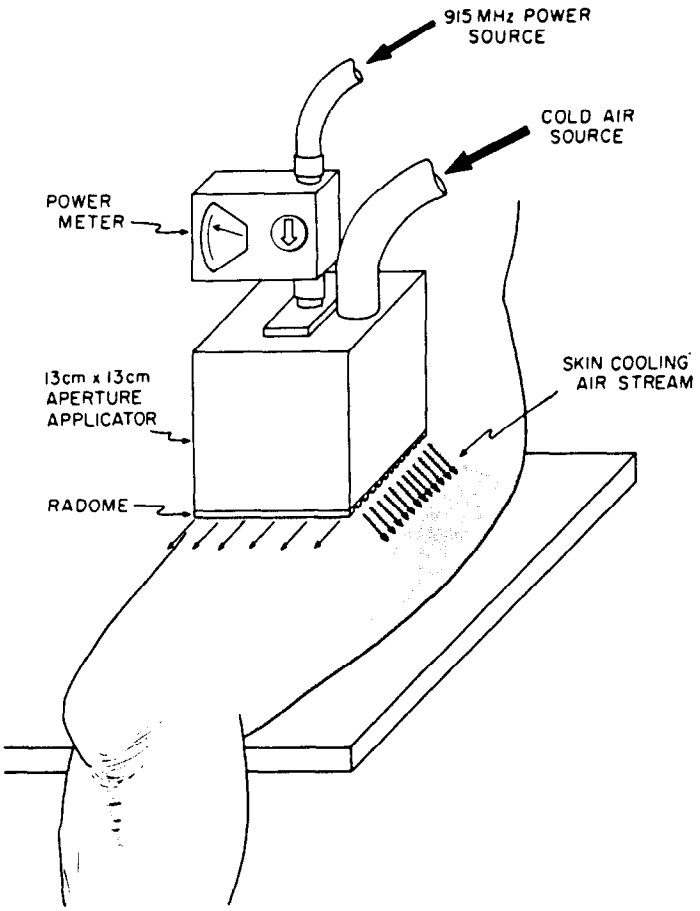

FIG. 3. Treatment of the anterior thigh with a 915 MHz, direct contact diathermy applicator.

BASAL TEMPERATURE PROFILE

In contrast to the usual thermal system, the body is not a heat engine since the metabolic generation is a by-product of the chemical reactions, primarily those occurring in muscle tissue, not the prime function of the body. All of the metabolically generated heat must be lost to maintain the body in thermal equilibrium. With the exception of a small loss by respiration, most (90%) of the heat loss occurs at the skin surface. The tissue temperatures are maintained at levels which are biologically safe and which yield optimal chemical reactions by the thermoregulatory system which adjusts these levels by varying the proportion of heat conducted and convected to the skin. The basal temperature profile is thus determined by the conduction of heat through the tissue to the skin, by convection through the blood flow to the skin and by the surface heat transfer. Whereas the arterial and deep tissue temperatures (rectal) are a result of the entire body's metabolic generation, the profiles in the tissues underlying the skin are more dependent upon the arterial blood temperature than upon the local metabolism.

Figure 4 illustrates the temperature profiles to be expected in a thigh for several different conditions. For all cases, the temperature of the interior sheath of the muscle was maintained at 36.5°C. Curve 1 represents the usual conduction profile; curve 2, the temperature due to local metabolism. It is interesting to note that the local metabolically generated heat produces an insignificant temperature rise. The rest of the curves illustrate different combinations of metabolism and blood flow. As shown, the energy convected by the blood dominates the temperature profile and substantial changes in the temperature levels are associated with small changes in the perfusion rate. The table on Fig. 4 lists the percentage of the heat lost from the skin surface which is contributed by conduction from the core, convection by blood, and local metabolism. For most cases, the energy carried from the core of the body to the skin by the blood supplies almost all of the energy lost from the surface. Thus small changes in the arterial supply temperature or the blood flow rate will produce substantial and significant changes in the entire temperature profile.

The two remaining important constituents of the

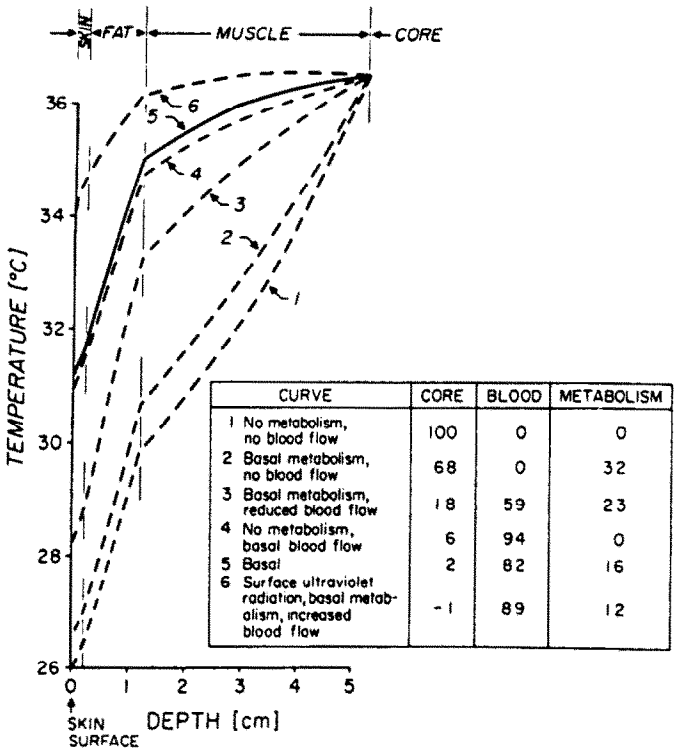

CURVE	CORE	BLOOD	METABOLISM
1 No metabolism, no blood flow	100	0	0
2 Basal metabolism, no blood flow	68	0	32
3 Basal metabolism, reduced blood flow	18	59	23
4 No metabolism, basal blood flow	6	94	0
5 Basal	2	82	16
6 Surface ultraviolet radiation, basal metabolism, increased blood flow	-1	89	12

FIG. 4. Temperature profiles for the cylindrical thigh model showing the effects of variations in metabolic heat generation and blood flow (h_s = 1.5 mW cm^{-2}°C^{-1}).

thermal profile are the fat thickness and surface heat transfer coefficients. Figures 5 and 6 illustrate these effects. Changes in the surface heat transfer coefficient cause substantial changes in the temperatures but, as expected, do not distort the basic shape. The major effect is in the skin temperature. It is interesting to note that, even in the worse case, the majority of the heat loss is still supplied by the blood and its portion is reasonably constant.

Figure 6 shows the effect of changing the fat thickness. The skin temperature and the temperature of the exiting blood (which is equal to the local tissue temperature because of the high effectiveness of the

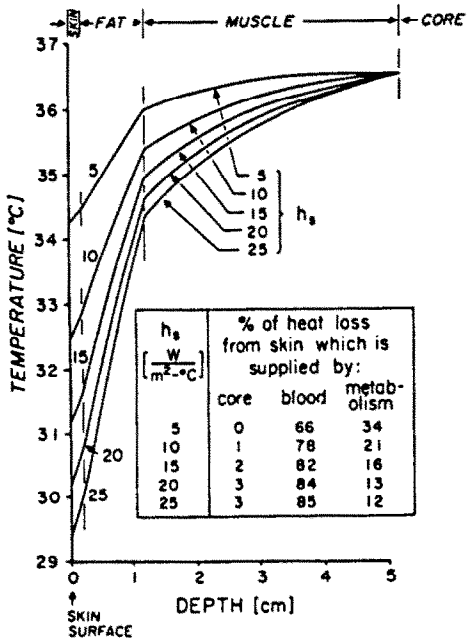

h_s $\left[\frac{W}{m^2 \cdot °C}\right]$	% of heat loss from skin which is supplied by: core	blood	metabolism
5	0	66	34
10	1	78	21
15	2	82	16
20	3	84	13
25	3	85	12

FIG. 5. Temperature profiles in the cylindrical thigh model showing the effect of the variation in surface convective heat transfer coefficients h_s.

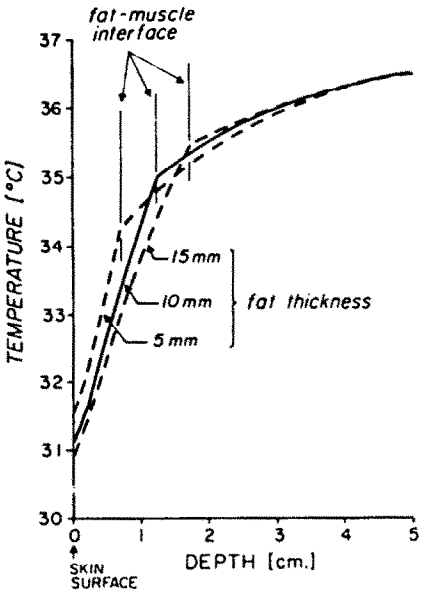

FIG. 6. Temperature profiles plotted vs depth.

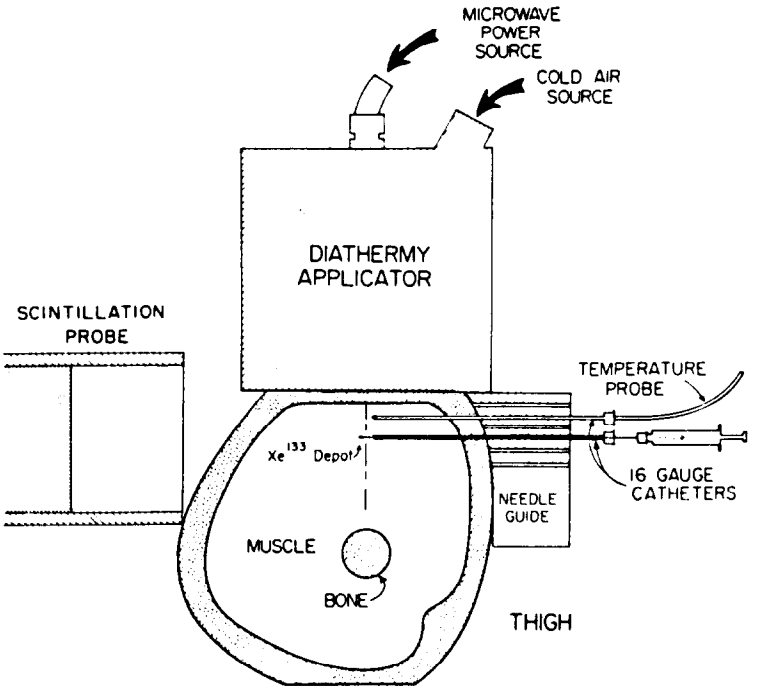

FIG. 7. Schematic of the experimental setup used to simultaneously study human muscle temperatures and blood flow rates.

vascular bed heat exchange) decrease while the muscle, fat and venous return temperatures increase. The thermoregulatory system, through its deep receptors, would sense the muscle temperature rise and call for vasodilation to eliminate more heat. On the other hand, the decreased skin temperature would lead to vasoconstriction. These contradictory responses are unlikely and it appears that some blood is shunted directly and laterally away from the superficial tissues. This is consonant with experimental data which show that an increase in fat thickness is accompanied by a decrease in fat perfusion [14].

EXPERIMENTS

As indicated by the results presented thus far, it is important that the local blood flow be known if any simulations are to be performed. At the same time, temperatures must be measured to determine if the simulations are correct.

To accomplish this, the experimental apparatus shown on Fig. 7 was used. A diathermy applicator, which included provisions for supplying cooled air to the skin surface, was placed on a subject's thigh. A needle guide was positioned alongside the thigh and used to guide 1–6 catheters such that their tips were at predetermined locations. Some of these contained special temperature sensors which were unaffected by the electromagnetic waves, while others contained hollow needles for injecting a radioactive tracer. An X-ray was taken of each thigh to measure the fat thickness, thigh shape and needle tip location. By injecting the Xe^{133} solution and measuring its washout rate with the scintillation counter, it was possible to determine the local blood flow rates [15]. Two series of tests were made. In the first, comprised of 44 tests upon 13 volunteer subjects, only blood flow measurements were made. In the second series, comprised of 15 tests on 15 subjects, both blood flow rates and temperatures were measured.

The washout was measured over a period as long as 20 min under: basal conditions; surface cooling; microwave heating; and combined surface cooling and microwave heating. Particular care was used to ensure that the time history of the Xe^{133} depot was an accurate indication of the blood flow rate. The mean resting blood flow rate (RBF) of 2.6 ml min^{-1} 100g^{-1} based upon tests with 28 thighs agrees well with other reported values (e.g. 2.6 ml min^{-1} 100g^{-1} [17]). The scatter in the RBF values is attributed to individual circulatory differences. In fact, individuals whose left and right thighs were both used showed a deviation of 0.28 ml min^{-1} 100g^{-1}. A slight correlation between the RBF and the ambient temperature was found, but since the ambient temperature was constant to within 2°C for all tests, the effect was not important.

Tests using surface cooling with 5°C air showed a mean muscle blood flow (MBF) decrease of 62 and 29% at the 1.5 and 3.0 cm depths, respectively after 5 min of cooling. When microwave heating was used alone, the increase in the MBF was found to be proportional to the time of heating and the microwave power. Tenfold increases were found at the 1.5 cm depth. When the surface was continuously cooled and microwave heating begun after 5 min of cooling, the superficial MBF was found to be nearly constant while

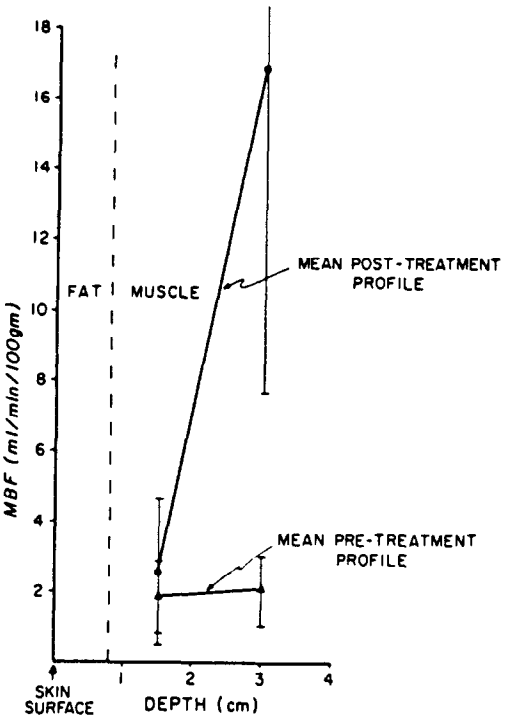

FIG. 8. Blood flow profiles in the thigh.

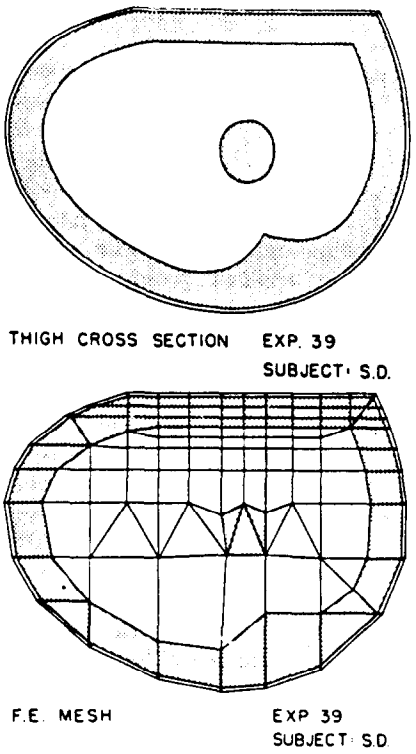

FIG. 9. Thigh cross section and finite element mesh for subject S.D.

the deep muscle *MBF* responded as indicated in Fig. 8. This figure clearly shows the ability of surface cooling to shift the therapeutic effects deeper into the tissue. The mean increase at 3 cm was 900% while at 1.5 cm it was 82%. In general, the *MBF* at 3 cm was tenfold that at 1.5 cm. By the use of surface cooling, the blood flow field appears to parallel the thigh temperature field in that a gradient of blood flow is established which is analagous to the temperature gradient.

THERMAL MODELLING OF THE THIGH

In order to estimate the effects of diathermy upon the local blood flow a series of numerical simulations were made. Figure 9(a) is a typical cross section of a thigh, distorted by the pressure of the applicator, and Fig. 9(b) indicates the corresponding finite element mesh used for the simulation. Acceptable simulation results were based upon the criterion that good agreement should exist between the predicted and measured temperature fields. This was done by manipulating the numerical estimate of the blood flow. When the predicted and measured temperatures were in good agreement, the estimated and measured flows were compared to determine if the blood flow model was reasonable. When both the temperature and the blood flows agreed, the simulation was complete and the model could then be used to predict the result of different treatment protocols. The following sections describe the different constituents of the simulation model.

The mesh and subjects

Six different subjects were tested. The diathermy applicator was placed on top of the thigh, flattening the upper surface as illustrated in Fig. 9. The different subjects had thin, medium and thick subcutaneous fat layers with fat thickness ranging from 0.33 to 1.85 cm. The mesh, Fig. 9(b), was composed of a densely constructed grid in the vicinity of the diathermy heated zone and a relatively sparse grid elsewhere with the exception of the surface. Since the surface heat transfer controls the tissue temperature field, relatively constant sized elements were used around the upper periphery of the thigh.

Thermal properties

Table 1 lists the thermal properties assigned to the different parts of the thigh [17]. These values were obtained from a comprehensive review of reported data. Although all other properties were taken as constants, the thermal conductivity of the fat was reduced when surface cooling began because of the effects of vaso constriction and counter-current cooling. Because the skin temperature reduction varies with fat thickness (Fig. 6), the fat thermal conductivity was reduced in proportion to the fat thickness. The minimum value was taken to be that of unperfused fat, 1.9 $W\,cm^{-1}\,C^{-1}$.

Table 1. Basal thermal properties

Tissue	k(mWcm^{-1}°C^{-1})	c(mJg^{-1}°C^{-1})	ρ(gcm^{-3})	f(mlmin^{-1} 100g^{-1})	$\dot{M}_0$(mWg^{-1})
skin	3.76	3770	1.0	9.8	1.0
fat	4.5	2300	0.85	2.75–10.0	0.32
muscle	6.42	3750	1.05	1.4–3.1	0.67
bone	1.16	1590	1.5	0.0	0.0
blood	5.49	3640	1.05		

Table 2. Arterial blood temperatures

Tissue	Thickness (cm)					
	0.32	0.55	1.0	1.11	1.55	1.85
fat	34.0	34.5	35.2	35.0	35.5	35.3
muscle	36.4	37.0	36.8	37.0	37.0	36.8

Basal blood perfusion

The energy supplied to the different nodes by the blood flow, namely,

$$f\rho c(T_a - T)$$

requires the specification of the perfusion rate, f, and the local arterial temperature, T_a. Through a series of numerical experiments, it was found that the best agreement with the measured basal temperature was achieved by assigning different values of T_a for the fat and for the muscle, as indicated in Table 2.

Microwave power deposition

The complex geometry of the thigh cross-section and that of the diathermy applicator preclude an accurate theoretical specification of the spatial distribution of the power deposited by the microwave field [SAR]. Using the method developed by Guy [18], the power deposition pattern was determined by microwave heating of a phantom model. These models were composed of split sections of materials which had the same dielectric properties as muscle, fat and bone. The models had the same cross section as the subject and were irradiated by the diathermy applicator, but at a very high power level. After a few seconds of radiation, and before any significant conduction of heat could occur, the two halves of the model were separated and a thermograph taken of their cross-sectional surface. If no conduction had occurred, or at most an insignificant amount, the thermographically recorded temperatures and the deposited power were related through

$$q_d''' = \rho c \frac{\Delta T}{\Delta t}.$$

Figure 10 illustrates a typical power deposition pattern. Figure 11 shows the deposition profile along the vertical axis of the thigh and a trough like deposition is seen in the fat. This type of deposition is due to a standing electromagnetic wave developed at the fat–muscle interface and was found only in the fatter subjects.

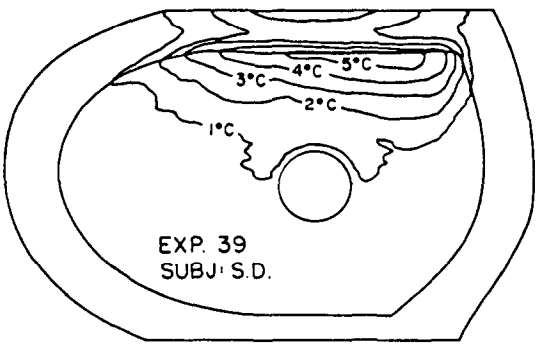

Fig. 10. EM deposition pattern in phantom model of subject S.D. in terms of temperature rise above ambient temperature.

Convective cooling conditions

While all the human experiments were performed under the same air flow and air temperature conditions, the different sizes and shapes of each thigh, as well as the variation from test to test in the areas of contact between the applicator and the thigh and of the air flow over the thigh, required that separate determinations of the surface heat transfer coefficients be made. Because of the very complex flow pattern at the skin surface, the surface heat transfer coefficients could only be approximately estimated and better values had to be determined experimentally. The phantom models were subjected to cooling and the temperature distributions measured at specified times. Finite element calculations were then made with different surface variations of the heat transfer coefficient until the predicted and measured temperature fields agreed. Values of h_s varied from 10 mW cm^{-2}°C^{-1} directly under the applicator to approx. 1 mW cm^{-2}°C^{-1} on the sides of the thigh.

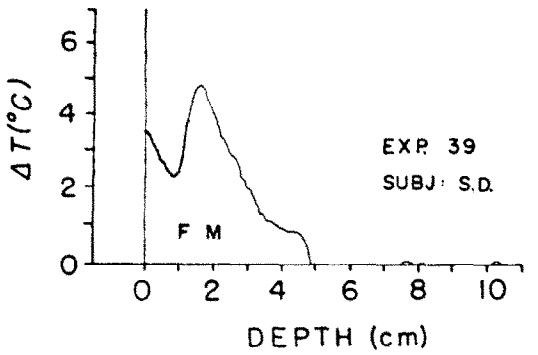

FIG. 11. Centerline depth profile of temperature rise ΔT in phantom model of subject S.D.

RESULTS OF THE THERMAL MODELLING

Temperatures

Figure 12 shows a typical comparison of the numerical simulation and the measured temperatures along the thigh centerline. In general, good agreement between the two was achieved, particularly in the heated region of the muscle. There were two systematic discrepancies which merit discussion. First, the experimental centerline skin temperatures were consistently below the numerically predicted values. These low values were caused by the necessity of locating the skin temperature thermistors on the skin in the centerline of the cooling air channel. Even though the thermistors made good contact with the skin, the usual problems of contact surface temperature measurements produced a consistent cooling bias of 2–3°C at the end of pre-cooling for all subjects. Second, it can be seen that the numerical power deposition for the fat layer temperature probe locations slightly overestimated the temperature as compared to that measured. This overestimate occurred in all the tests and was found only in the region of steep deposition [*SAR*] gradients. Errors associated with the thermographic measurements, heat conduction during the phantom tests, inexact correspondence between model and tissue properties and problems in precisely defining the probe tip position in the human subject are suspected to be the cause of the small differences. Figure 13 shows a comparison for the centerline of the cross-section as a function of depth for both the temperatures and the blood flow rates. The slight differences between the predicted and measured values are much better than usually expected when dealing with such poorly defined thermal properties as found in living tissue.

Blood flow modelling

To produce the good match between the predicted and measured temperatures required that a model of the blood flow suppression due to surface cooling and augmentation due to microwave heating be developed. Unfortunately, there is no such model, and we chose to use the simplest mechanism which produced acceptable results.

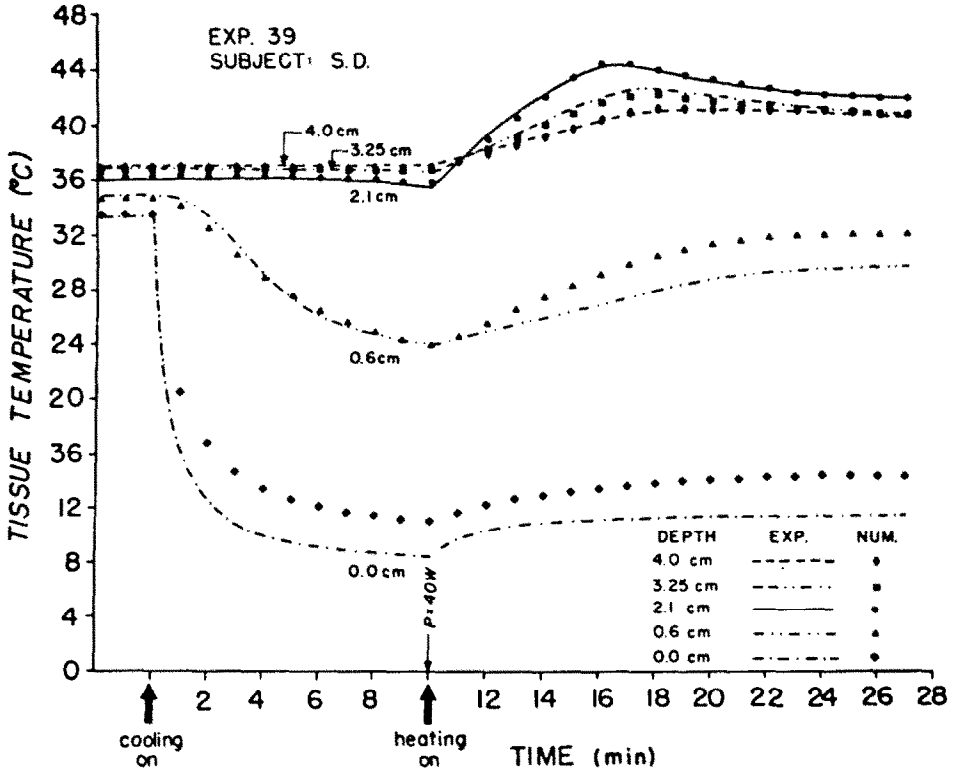

FIG. 12. Comparison of experimental (EXP) and numerically determined (NUM) transient temperature data at different depths for subject S.D.

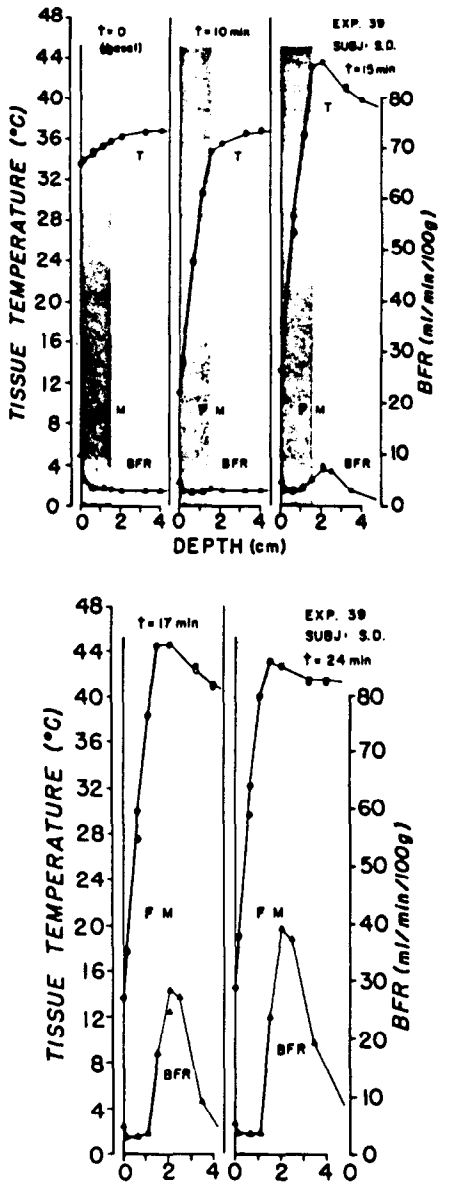

FIG. 13. Time sequence of numerical and experimental blood flow and temperature profiles occurring in subject S.D. The solid black symbols represent experimental data; open symbols represent numerical results. Shading denotes the fat layer.

1. *Blood flow model for cooling.* For the cooling of the skin, fat and superficial muscle we assumed a mechanism in which the blood flow was decreased from the initial values in proportion to the temperature reduction from the basal temperatures i.e.

$$f = f_0[1 - K(T_{basal} - T)] \quad (5)$$

where the proportionality constant, K, was different for the different materials. In general, variations in K for the skin were not important because of the very high skin conductance due to the small thickness. Conversely, the range of K for the fat was much smaller

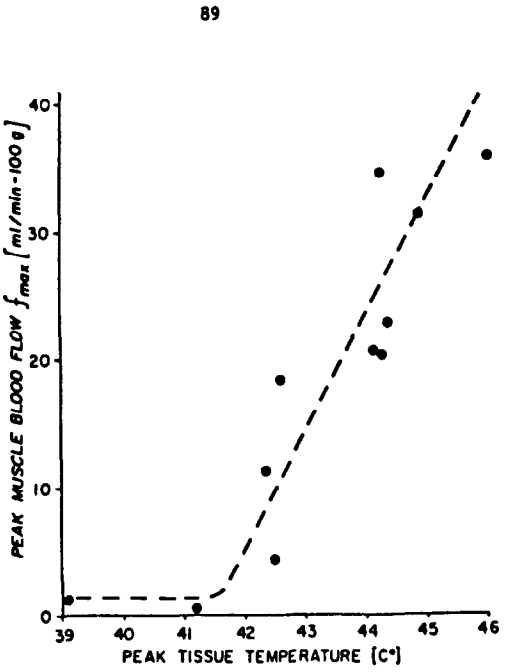

FIG. 14. The relationship between local peak tissue temperature at the Xe injection site and the maximum measured blood flow.

(0.01–0.035) due to the increased sensitivity of the temperature profiles because of the relatively greater thickness of the fat layer in comparison with the skin. The fatter subjects, and thus the better insulated subjects, showed a much smaller reduction in blood flow than did the thin and poorly insulated subjects.

This concept is admittedly oversimplified, since one should also include the effects of shunting and of reduced arterial temperatures due to counter current heat exchange with the colder returning blood. Data from the first series of blood tests showed that the blood flow in the shallow muscle layers was reduced and that the returning blood was much cooler. The second series of blood tests showed that the colder blood returning from the shallow layers continued to cool the deeper muscles (2 cm) for several minutes after

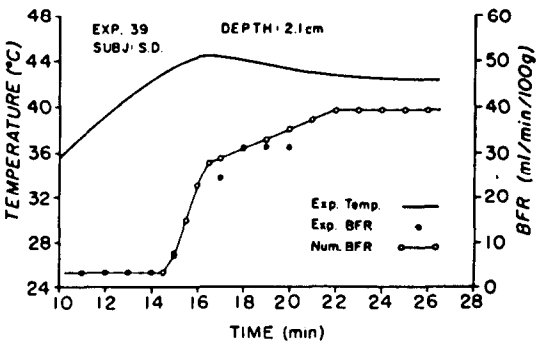

FIG. 15. The transient temperature and experimental and numerical blood flow response occurring at the site of the xenon injection depot for subject S.D.

the cooling had been shut off. In our case, all of these effects were lumped into K.

2. *Blood flow model for heating.* After the onset of microwave heating, the temperature of all nodes was monitored. Blood flow for nodes whose temperature remained below basal values was determined through equation (5). Blood flow in the skin and fat for nodes which exceeded the basal temperature was maintained at *RBF* since no human data has shown that either skin or fat have elevated perfusion rates [18]. Blood flow for the muscle nodes whose temperature increased sufficiently was increased in proportion to the experimentally determined critical temperature. Thus, using Fig. 1, when a node showed a sudden reduction of temperature, the blood flow was increased according to Fig. 14, using the degree of temperature elevation ($T_{critical} - T_{basal}$) to determine the amount of increased perfusion. Once the perfusion had been increased, it was maintained at its elevated value, even when the temperature subsequently decreased since experiments have shown that a substantial time is required before the flow rate returns to normal.

3. *Blood flow results.* The different parameters needed in the simulation were adjusted until the measured and predicted temperatures were in the best agreement. At this point, a comparison was made of the measured and predicted blood flow rates as illustrated in Fig. 15. Some of the comparisons were not as satisfactory as the one shown for several reasons: (1) the washout data derived from the washout measurements is not ideally suited to measuring rapid changes because of the need for counting the gamma ray events over a minimum 1 min period; (2) Xe^{133} clearance is measured over a volume not a point in the tissue; (3) frequently the xenon clearance was complete before the time of maximum blood flow.

In any respect, the agreement is much better than any determined previously and especially when considering the difficulties of measurement and the diffuse nature of the physiological response of the body. It is interesting to note that while previous estimates of maximum blood flow have been in the range of 30–40 ml min^{-1} 100 g^{-1}, values in excess of 70 were predicted. Such high values are supported by some recent work of Grimby [20] who measured values as high as 65 during exercise.

Steady state results

Figure 16 shows the numerical near-steady state results for the six subjects tested. The appearance of the *SAR* and *BFR* curves are similar in shape, although the *BFR* curves are shifted inward relative to the *SAR* curves. It is particularly interesting to note that the blood flow may be depressed in the region of maximum temperature and the maximum blood flow may be found at tissue temperatures below the usually defined critical temperature of 42°C (see also Fig. 14).

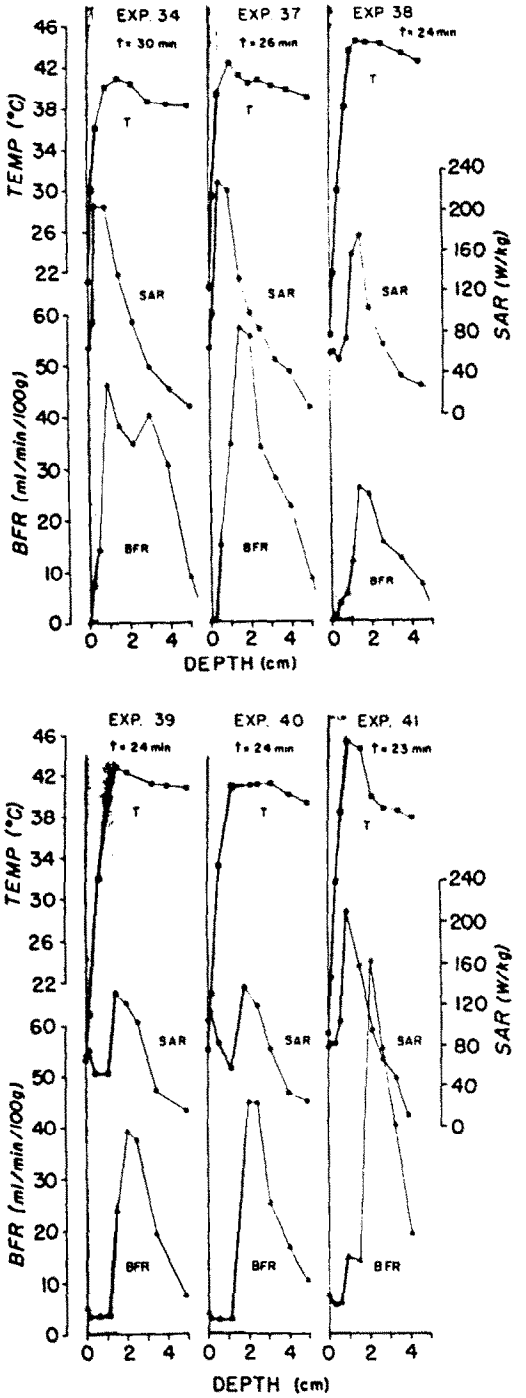

FIG. 16. The numerical values of the steady state temperature, *SAR* and *BFR* profiles. The shading denotes the fat layer.

TUMOR TREATMENTS

When a tumor is present below the skin surface, there are often areas of increased skin temperature in comparison with normal tissue in the diseased region [22]. This region of increased temperature is due primarily to the increased heat deposited by the elevated blood flow in the tumor. Correct diagnosis by skin thermography requires an accurate interpretation of the skin temperature distribution. Figure 17(a) illustrates two hypothetical cases. Using the finite

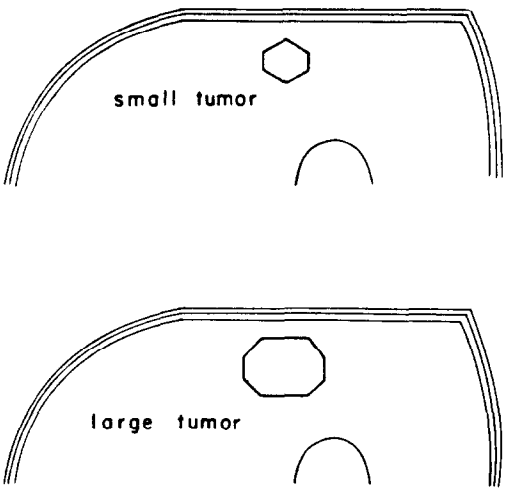

Fig. 17(a). Cancer models constructed by placing tumor regions of elevated blood flow ($4 \times RBF$) in the thigh model.

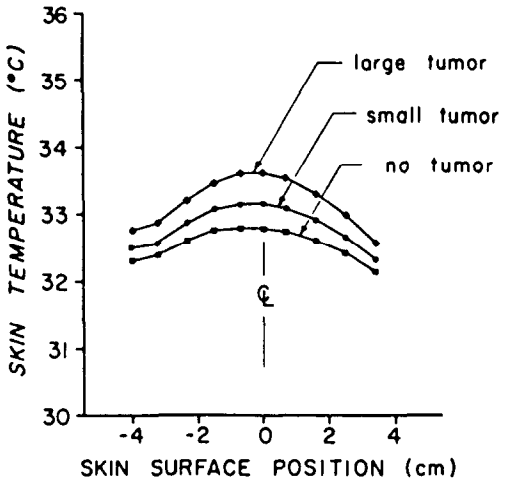

Fig. 17(b). The effect of the presence of the tumors on the skin temperature distribution.

element model, with a perfusion rate in the tumor of 4 times the normal rate, the skin temperature distributions of Fig. 17(b) were found. The distinct differences between the three different cases suggest that a thermal analysis may be used to determine the rate of heat generation in a tumor whose size and location has been determined by X-ray. Such heat generation may provide valuable information as to its type, rate of metabolism and growth. The thermal analysis may also be used to estimate the correct thermal dose, i.e. the product of elevated temperature and time, to be used. Figure 18 illustrates the difference in the temperatures produced by two different power levels. Not only are the temperatures higher for the 60 W dose, but the entire tumor is at an elevated temperature. By contrast, in the 40 W dose, most of the tumor is not at an elevated temperature and it is possible that the deposited energy will be of little or no therapeutic value.

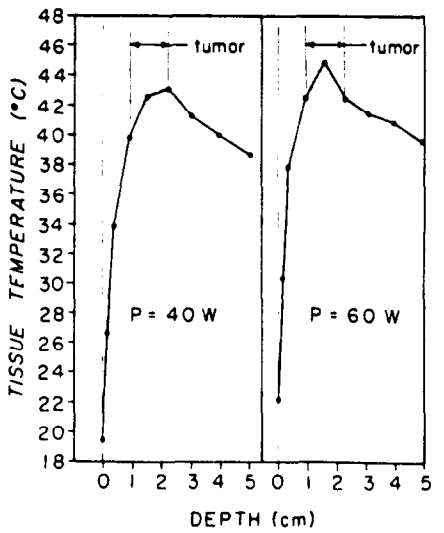

Fig. 18. Comparison of the steady state hyperthermic regions in the small tumor due to diathermy treatment at two different absorbed power levels. Shaded regions indicate relative thermal toxicity of the treatments.

CONCLUSIONS

Numerical simulation is used in two ways. First to determine if a specific parameter is correct or if a mechanistic model is sufficient to yield results which agree with experimental data. Second, to extend experimental results to situations which are either difficult or possibly impossible to model. In this paper, we have given examples of both of these uses. The verification of the simulation, while not as exact as is common in heat transfer research, should be regarded as particularly good when one considers the difficulty in accurately defining the thermal properties of living tissue. The simple temperature-blood flow model used is not proposed to be the true physiological mechanism but in the specific tests conducted it mimicked our data and was sufficient to give good simulation of the complex phenomena associated with diathermy. The simulation also clarified the dominant roles of blood perfusion and fat thickness in establishing the basal temperature distribution.

By using the simulation technique, the importance of the local blood flow, and its constriction by surface cooling, in establishing effective diathermy protocols was emphasized. The technique can be used, as demonstrated by the example, to define the time–dose relationship needed to provide useful treatment of deep muscle tissue or thermosensitive tumors.

Eventually, through the cooperation of heat transfer specialists and medical practitioners, it may be possible to routinely use thermal analyzers to define ideal treatment protocols for diathermy and for any other medical treatment which involves the use of heating or cooling modalities.

Acknowledgement—This work was supported in part by grant 16-P-56818 Rehabilitation Service Administration, U.S. Department of Health, Education and Welfare.

REFERENCES

1. A. W. Richardson, C. G. Imig, B. L. Feucht and H. M. Hines, Relationship between deep tissue temperature and blood flow during electromagnetic irradiation, *Archs Phys. Med.* **31**, 19–25 (1950).
2. S. Szmigielski, M. Bielec, M. Janiak, M. Kobus, M. Luczak and E. DeClercq, Inhibition of tumor growth in mice by microwave hyperthermia, polyriboinosinic-polyribocytidylic and mouse interferon, *IEEE Trans. Microwave Theory and Techniques*, MTT 26, pp. 520–522 (1978).
3. W. G. Connor, E. W. Gerner, R. C. Miller and M. L. M. Boone, Prospects for hyperthermia in human cancer therapy, *Radiology* **123**, 497–503 (1977).
4. J. F. Lehmann, Diathermy, Chap. 11 in *Handbook of Physical Medicine and Rehabilitation*, 2nd Ed., (edited by F. H. Krusen, F. J. Kottke and P. M. Ellwood) pp. 27. W. B. Saunders, Philadelphia (1971).
5. J. F. Lehmann, G. D. Brunner, J. A. McMillan, D. R. Silverman and V. C. Johnston, Modification of heating patterns produced by microwaves at frequencies of 2456 and 900 Mc by physiological factors in the human, *Archs Phys. Med. Rehabil.* **11**, 555–563 (1964).
6. J. F. Lehmann, D. R. Silverman, B. F. Baum, N. L. Kirk and V. C. Johnston, Temperature distributions in the human thigh, produced by infrared, hot pack and microwave application, *Archs Phys. Med. Rehabil.* **56**, 442–448 (1975).
7. J. F. Lehmann, B. J. deLateur and J. B. Stonebridge, Heating patterns produced in humans by 433.92 MHz round field applicator and 915 MHz contact applicator, *Archs Phys. Med. Rehabil.* **56**, 442–448 (1975).
8. A. W. Guy, J. F. Lehmann, J. B. Stonebridge and C. C. Sorensen, Development of a 915 MHz direct contact applicator for therapeutic heating of tissues, *IEEE Trans. Microwave Theory and Techniques*, MTT 26, 550–556 (1978).
9. L. A. Newburgh, *Physiology of Heat Regulation and the Science of Clothing*, Hafner, New York (1968).
10. A. F. Emery and K. M. Sekins, Computer modeling of thermotherapy, Chapter 4 in *Therapeutic Applications of Heat and Cold*, (edited by J. F. Lehman) Williams and Wilkins, New York (1981).
11. J. C. Chato, Heat transfer to blood vessels, ASME paper 79-WA/HT-68 (1979).
12. W. Perl, Heat and matter distribution in body tissue and the determination of tissue blood flow by local clearance methods, *J. Theoret. Biol.* **2**, 201–235 (1962).
13. H. A. Pennes, Analysis of tissue and arterial blood temperatures in the resting human forearm, *J. Appl. Physiol.* **1**, 93–122 (1948).
14. O. A. Larsen, N. A. Lassen and F. Quaade, Blood flow through human adipose tissue determined with radioactive Xenon, *Acta Physiol. Scand.* **66**, 337–345 (1966).
15. H. Hovind and S. L. Nielsen, Changes in subcutaneous and muscle blood flow after shortwave diathermy, *Proc. 7th European Conf. Microcirculation*, Aberdeen, pp. 417–422 (1972).
16. C. A. Keele and E. Neil (eds) *Samson Wright's Applied Physiology*, pp. 62, 149. Oxford University Press, London (1971).
17. K. M. Sekins, Microwave hyperthermia in human muscle: An experimental and numerical investigation of the temperature and blood flow fields occurring during 915 MHz diathermy. Ph.D. Thesis, University of Washington (1981).
18. A. W. Guy, Analysis of electromagnetic fields induced in biological tissues by thermographic studies on equivalent phantom models, *IEEE Trans. Microwave Theory and Techniques*, MTT 19, pp. 205–214, (1971).
19. G. Grimby, E. Haggendal and B. Saltin, Local Xenon 133 clearance from the quadriceps muscle during exercise in man, *J. Appl. Physiol.* **22**, 305–310 (1967).
20. J. W. Draper and J. W. Boag, The calculation of skin temperature distributions in thermography, *Physics Med. Biol.* **16**, 201–211 (1971).

UTILISATION DES PRINCIPES DE LA THERMIQUE POUR OPTIMISATION DES MODALITES DE TRAITEMENT DE LA DIATHERMIE ET DU CANCER

Résumé—On décrit une étude expérimentale et numérique de la réponse thermique d'une cuisse humaine exposée aux traitements diathermiques. En faisant varier les paramètres de simulation et le modèle de température du sang en écoulement, il est possible d'obtenir un bon accord entre les températures calculées et mesurées et les débits sanguins. La technique de simulation peut être utilisée pour prédire la réponse d'un tissu vivant à une variété de traitements. Un exemple est donné par l'application de la méthode à la définition de la dose diathermique correcte pour le traitement d'une tumeur.

DIE ANWENDUNG VON WÄRMEÜBERTRAGUNGSPRINZIPIEN BEI DER KONSTRUKTION VON OPTIMALEN DIATHERMIE- UND KREBSBEHANDLUNGSGERÄTEN

Zusammenfassung—Es wird eine experimentelle und numerische Studie des thermischen Verhaltens eines menschlichen Oberschenkels beschrieben, der einer Diathermie-Behandlung ausgesetzt ist. Bei einer geeigneten Variation der Simulationsparameter und des temperaturabhängigen Blutströmungsmodells ist es möglich, eine gute Übereinstimmung zwischen den berechneten und gemessenen Temperaturen und Durchblutungsraten zu erhalten. Die Simulationstechnik kann ferner dazu benutzt werden, die Reaktion des lebenden Gewebes auf eine Vielzahl von Behandlungsabläufen vorauszubestimmen. Als Anwendungsbeispiel wird die Bestimmung der richtigen Strahlendosis für eine Tumorbehandlung gegeben.

ИСПОЛЬЗОВАНИЕ ЗАКОНОВ ТЕПЛОПЕРЕНОСА ДЛЯ ОПТИМИЗАЦИИ ДИАТЕРМИИ И РАЗРАБОТКИ МЕТОДИКИ ЛЕЧЕНИЯ РАКА

Аннотация — Описано экспериментальное и численное исследование скорости роста температуры в бедре человека при диатермии. Меняя нужным образом параметры модели и сами модели, имитирующие поток крови, можно получить хорошее согласие между расчетными и измеренными значениями температуры и скорости тока крови. Эта методика может использоваться для определения реакции живой ткани на различные методы лечения. Приведен пример использования метода для определения дозы диатермии при лечении опухоли.